

See discussions, stats, and author profiles for this publication at: <https://www.researchgate.net/publication/302415604>

# The effects of jet plume configuration on the installation efficiency of jet fans

Conference Paper · October 1997

---

CITATION

1

READS

24

4 authors, including:



Mohammad Tabarra

Arup

36 PUBLICATIONS 20 CITATIONS

SEE PROFILE

Some of the authors of this publication are also working on these related projects:



Aerodynamic drag of vehicles in tunnels [View project](#)



Sustainable Design of Metro Stations [View project](#)

Extract from 9th International Symposium on  
"Aerodynamics & Ventilation of Vehicle Tunnels", BHRG, Italy, Oct 97,  
MEP Vol. 27, ISBN 1860580920 pp 57-76

## The effects of jet plume configuration on the installation efficiency of jet fans

W T W CORY

Woods of Colchester

R D MATTHEWS, M TABARRA, and B KENRICK

Centre for Tunnel Aerodynamics Research, South Bank University

### SYNOPSIS

A comprehensive series of tests were carried out on a 1/15 scale model of a simplified rectangular vehicle tunnel in order to investigate the effects of jet swirl, separation from tunnel roof, inclination and hub to tip (h-t) ratio on installation efficiency. A 64mm diameter pipe fed by a centrifugal fan positioned at the tunnel portal was used to simulate a jet fan.

Velocity measurements were made at the exit portal of the tunnel for different positions of the jet at the tunnel entrance. Swirl effects were examined by comparing installation efficiencies of the jet with 0°, 17°, 30° of swirl induced by guide vanes. The effect of h-t ratios of 0, 0.25, 0.5, 0.72 and jet inclinations of 0°, 5°, 10°, 15° were examined. All tests had a constant mass flow rate.

Separation from the wall to the tunnel centre resulted in efficiencies of 88% - 100% in the zero hub, zero swirl case. The 0.25 h-t ratio tests with 0°, 17°, 30° swirl were grouped together with efficiencies in the 84-85% at the wall and 95-96% at the centre, implying that swirl has a negligible effect for zero pitch configuration. Increasing the h-t ratio to 0.72 caused the efficiency to drop to 71% at the wall and 80% at the centre.

## Nomenclature

### Roman Symbols

a	Jet Area	H	Tunnel Height
A	Tunnel Area	k	Minor Losses
Ct	Craya-Curtet Number	l	Length
D	Diameter	M	Momentum
D <sub>h</sub>	Hydraulic Diameter	P	Pressure
F	Force	S	Separation
f	Friction Factor	V	Velocity

### Greek Symbols

ρ	Air Density	sec	Secondary
α	Area Ratio (a/A)	T	Tunnel
ω	Velocity Ratio (V <sub>jet</sub> /V <sub>T</sub> )	j	Jet
η	Efficiency	cl	Centre-line
τ	Shear Stress	w	Wall

### Subscripts

sec	Secondary
T	Tunnel
j	Jet
cl	Centre-line
w	Wall

## 1. Introduction.

As part of a comprehensive investigation of jet fan installation effects work has been carried out in conjunction with Woods of Colchester at South Bank University CentTAR (1,2) examining the installation efficiency of circular air jets directed along a rectangular duct or tunnel. While the jets were effectively ejectors rather than jet fans their cross section was circular and they had a range of centre body sizes supported by guide vanes some of which imparted swirl to the resulting annular jet. A few of the jet configurations of "Hub/tip" ratio and swirl angle were an approximation of some jet fan values.

The basic experimental configuration is shown in Fig. 1, where the rate of change of jet momentum is balanced by the frictional forces on the bulk tunnel flow. The friction forces are in turn proportional to the tunnel mean dynamic pressure  $\frac{1}{2}\rho V_T^2$  and the momentum equation can be written as:

$$\alpha\omega^2 - \alpha\omega - \beta = 0$$

where  $\omega$  is the jet to tunnel velocity ratio

$\alpha$  is the jet to tunnel area ratio

$\beta$  is the system pressure loss coefficient referred to  $\rho V_T^2$

Under these ideal or equilibrium conditions the resulting velocity ratio will be given by

$$\omega = 0.5 + \left\{ 0.25 + \frac{\beta}{\alpha} \right\}^{\frac{1}{2}}$$

In practice the diffusion of a circular jet in a tunnel is complex and will always involve wall shear stresses  $\tau_w$  in excess of those given by  $\tau_w = f \frac{1}{2} \rho V_T^2$  where  $f$  is the friction factor.

Circular jets are rarely truly axisymmetric and will often entrain mass flow asymmetrically such that their centre line will tend to curve as they diffuse. This effect is compounded by the proximity of the tunnel wall and the coanda effect so that there is always the probability for a full size jet or the jet in the test facility used in this project the jet will wander or curve towards the 'roof' or 'floor' even when the jet is nominally in the centre of the tunnel.

Under these circumstances local velocities adjacent to the wall will be in excess of the tunnel velocity  $V_T$  with consequent increased values of local shear stress. Losses will therefore always be greater than the simple Darcy values. Velocity ratios will therefore always be greater than the ideal value which for a fixed jet velocity  $V_j$  implies a reduced tunnel velocity  $V_T$ . This reduced effectiveness is allowed for by defining an installation efficiency  $\eta_i$  as

$$\eta_i = \frac{\beta}{\alpha\omega^2 - \alpha\omega}$$

Having estimated  $\beta$  allowing for any entry and exit losses and Darcy friction, measurements of the actual value of  $\omega$  will allow the installation efficiency to be calculated for a given jet size.

The general methodology reported here is basically concerned with measuring  $\beta$ ,  $\alpha$  and  $\omega$  and from them inferring the installation efficiency for a particular jet configuration. It is worth noting at this stage that the installation efficiency is very dependant on accurate measurements but most especially on the tunnel velocity  $V_T$ .

## 2. Experimental Study

The experimental program was carried out to determine the influence of wall proximity, swirl, jet momentum and inclination on installation efficiency as defined above. The tunnel at South Bank University consisted of a 1/15th scale model of a simplified rectangular vehicle tunnel, width 0.55 m and height 0.3 m. The model corresponds to a two-lane cut and cover tunnel of height 4.5 m and width 8.25 m. For the experiments a tunnel length of 13.45 m was used. An initial investigation was carried out using various nozzles with and without centre bodies but all mounted in the centre of the tunnel near the inlet plane. The jets were supplied by a centrifugal fan. The jet mass flow was measured via an orifice plate positioned half way along the pipe down stream of the centrifugal fan (3).

The main body of the experimental work consisted of various configurations of jet eccentricity which were tested together with various degrees of swirl, hub to tip ratio and jet inclination to the wall. The test series were of two main types, the first involved jet separation from the tunnel roof (R tests) and the second from the wall-roof corner (C tests). The jet separation is in non-dimensional terms of separation of the jet edge from the wall S and the tunnel height H.

Jet separation is  $\frac{S}{H}$  and varies from a minimum of 0.0169 at the tunnel roof to a maximum of 1 at the tunnel centre. The swirl tests were only carried out for a 0.25 hub to tip ratio with average swirl angles of 17° and 30°.

The jet momentum tests were carried out using plane jets of diameter 31 mm, 52 mm and 64 mm and annular jets in a 64 mm diameter duct containing centre bodies of 16 mm, 32 mm and 46 mm diameter. All swirl and momentum tests were carried out for nine eccentricities from the tunnel wall (R) and eight eccentricities from the wall-roof corner (C) towards the tunnel centre. The jet inclination tests were carried out on each swirl and momentum condition for angles of 0°, 5°, 10° and 15° for three eccentricities from the wall and two eccentricities from the wall-roof corner.

The test matrices are shown on the tables below.

Table 1. The test matrix to study the effect of swirl and separation and wall separation  
Hub/Tip = 0.25 ratio only.

$\frac{H-D_c}{2}$	Swirl				Angle			
	0°	17°	30°		0°	17°	30°	
0.01695	R-C	R-C	R-C	R	R-C	R-C	R-C	R
0.03389	R	R	R	R	R-C	R-C	R-C	R
0.06779	R-C	R-C	R-C	R	R	R	R	R
0.13559	R	R	R	R	R	R	R	R
0.27118	R-C	R-C	R-C	R	R-C	R-C	R-C	R
0.40678	R-C	R-C	R-C	R	R-C	R-C	R-C	R
0.54237	R-C	R-C	R-C	R	R-C	R-C	R-C	R
0.67797	C	C	C	C	C	C	C	C
0.81356	R-C	R-C	R-C	R	R-C	R-C	R-C	R
1	R-C	R-C	R-C	R	R-C	R-C	R-C	R

Table 2. The test matrix to study the effect of hub to tip ratio (jet momentum) and wall separation.

$\frac{H-D_c}{2}$	Hub to Tip Ratio			
	0 to 1	0.25 to 0.5	0.5 to 0.72	0.72 to 1
0.01695	R-C	R-C	R-C	R-C
0.03389	R	R	R	R
0.06779	R-C	R-C	R-C	R-C
0.13559	R	R	R	R
0.27118	R-C	R-C	R-C	R-C
0.40678	R-C	R-C	R-C	R-C
0.54237	R-C	R-C	R-C	R-C
0.67797	C	C	C	C
0.81356	R-C	R-C	R-C	R-C
1	R-C	R-C	R-C	R-C

Table 3. Test matrix to study the effect of jet inclination and wall separation (tests carried out on all swirl and momentum conditions).

$\frac{H-D_c}{2}$	Angle Of Incline			
	0°	5°	10°	15°
0.01695	R-C	R-C	R-C	R-C
0.27118	R-C	R	R	R
0.54237	R-C	R-C	R-C	R-C

Velocity measurements were recorded using a Laser Doppler Anemometer (LDA). The LDA used was a Dantec two component type based on a 300 mW Argon Ion laser with a Bragg cell shift for measuring the direction of flow. The front lens focal length was 600 mm and the measurement volume was of diameter 0.16 mm and length 2.4 mm. Particles of atomised olive oil were injected into the flow stream. The correlation processor attached to the optics logged the data from the probe directly to the hard disc of a PC, which records the particle velocity, its arrival time and transit time through the measurement volume.

The flow velocity was measured at 224 points across the duct at the exit portal (based on a 16 x 14 point matrix) as depicted in Fig. 2. The measurement points were concentrated at the tunnel roof, floor and walls in order to capture the velocity gradients in the boundary layer. The velocity gradient at the centre of the duct was sufficiently low that fewer measurement points were required to measure it accurately. After completion of the experiment mean velocity values were computed for each traverse point.

In all tests an average local velocity was calculated from 2,000 samples taken at each measurement point. The flow rate was established by integrating across the exit portal assuming a zero velocity at the duct walls. The tunnel average velocity was calculated as a proportion of the centre line velocity to reduce test times in later experiments. Atmospheric pressure and local air temperature were recorded as each test was conducted.

### 3. Experimental Programme.

The experimental investigation required a good knowledge of the allowable ventilation losses  $\beta$  and the tunnel velocity  $V_T$  (and hence) for all configurations in order to calculate the installation efficiencies.

The system losses which can be determined with some accuracy are made up of the Darcy friction losses and the portal entry and exit losses. The portal entry loss was small and was not separately measured for this experiment but absorbed in a bulk entry/exit loss.

Tests were carried out to determine friction factor and relative roughness by plotting static pressure distribution down the tunnel at a measured value of  $V_T$ . From these measurements relative roughness was determined and the ventilation flow loss coefficient was calculated and plotted as a function of tunnel velocity  $V_T$ .

A second preliminary investigation was carried out to examine the tunnel exit velocity profile to ensure that the jet momentum was fully diffused and that the three dimensional velocity profiles for  $V_T$  at tunnel exit were similar for various values of average tunnel velocity.

To determine the installation efficiency for all the jet configurations the study was conducted in two parts. For the first set of tests the jet configuration was maintained parallel to the tunnel axis ( $0^\circ$  inclination) while being moved from the tunnel centre towards the roof, and then from the roof-wall corner towards the tunnel centre as depicted in Fig. 3. For each configuration, the total tunnel mass flow was recorded by a point traverse at the tunnel outlet with the laser anemometer. From this the relationship between the centre point velocity ( $V_{cl}$ ) at the exit portal and the average tunnel velocity ( $V_T$ ) was established (see Fig. 4). The tunnel length was 34.6 hydraulic diameters and to speed the experimental procedure it was assumed that the exit velocity profile was fully developed and similar for each configuration. This assumption implies that the ratio of  $V_{cl}/V_T$  remains constant for each configuration and jet momentum. Figure 4 shows an approximate straight line relationship with a best fit line through the data points having a slope of 0.847. The  $V_{cl}$  at the exit portal was recorded at different jet separations, hub to tip ratios and with the jet angled away from the tunnel roof and roof-wall corner at  $5^\circ$ ,  $10^\circ$ ,  $15^\circ$  as depicted in Figs 5a and 5b. The primary jet mass flow was kept constant for all eccentricity tests.

#### 4. Results.

The first result to consider has already been presented in Fig. 4 and showed the straight line relationship between average tunnel velocity  $V_T$  obtained by full integration of the three dimensional velocity profile and the tunnel centre line value. This established a useful empirical relationship between centre line velocity and the average tunnel velocity for this test facility as

$$V_T = 0.847 V_{cl} - 0.0625$$

The second important result obtained was the loss factor determined from streamline static pressure measurements taken at the highest value of  $V_T$ . From these measurements a value of relative roughness was determined as 0.0012 for the test facility. The loss factor for the momentum equation then becomes

$$\beta = 69.29f + 0.58 \text{ for flared entry and sudden exit}$$

$$\text{or } \beta = 69.29f + 0.60 \text{ for plane entry and sudden exit.}$$

The tunnel loss coefficients  $\beta$  are shown in Fig. 6 plotted against tunnel velocity.

The first test carried out was to position each nozzle in turn in the centre of the tunnel to determine the reference value of installation efficiency. The results are shown in Fig. 7.

Two features of Fig. 7 are worth noting, the first concerns the way that the installation efficiency of a plane jet (no centre body) increases slightly with jet velocity (1) while the second feature is the loss of installation efficiency associated with annular jets of the same area and velocity ratios as the plane jets. It is suspected that this is due to very rapid diffusion of

the annular jet 'filling in' its low velocity core without rapidly reducing its nominal annular velocity to the equivalent plane jet velocity based on the jets outer dimensions. More work is required on this effect. It is noted that most jet fan installations involve 1D or 2D silencers with jet velocities and associated thrusts referred to the plane jet values at the silencer exit plane.

The installation efficiencies for the jet positioned parallel to the tunnel axis are shown in Figs 8 and 9. Fig. 8 shows the effect of separation away from the roof while Fig. 9 shows the effect of jet separation from the wall-roof corner towards the tunnel centre point. As the separation from the roof increases the installation efficiency increases, reaching a maximum when the jet is at the centre of the tunnel. The plane jet (i.e. no centre body, no swirl) demonstrates the highest efficiency ranging from 88% at the wall to 100% at the tunnel centre.

The three sets of swirl test results are also shown in Figs 8 and 9. They are all for a hub-tip ratio of 0.25 (16 mm diameter centre body) but having mean exit swirl angles of  $0^\circ$ ,  $17^\circ$  and  $30^\circ$ . It is noted that there is no discernible effect of swirl on installation efficiencies for these tests with zero pitch configuration.

From the test results there is no evidence that a swirling jet diffuses x-momentum along the tunnel more efficiently into the secondary flow or that secondary flow entrainment is in any way enhanced.

The increased jet momentum created with a 0.5 h-t ratio (32 mm diameter centre body) resulted in efficiencies ranging from 81% at the roof to 91% at the tunnel centre. The lowest efficiencies were recorded while using a 0.72 h-t ratio (46 mm diameter centre body), the substantial increase in jet momentum resulted in efficiencies of 71% at the wall increasing to 80% at the tunnel centre. The decrease in efficiency with increased momentum is thought to be caused by the filling in of the annular jet mentioned earlier.

The installation efficiencies for the jet in the corner are approximately 10% lower than those with the jet adjacent to the roof and converge with increased separation to identical values at the tunnel centre. The installation efficiencies for the corner tests are understandably lower because of the increased shear caused by having two adjacent surfaces.

The jet pitch angle tests (roof configuration) and pitch-yaw angle tests (corner configuration) are shown in Figs 10 to 21; even numbers are pitch angle results and odd numbers are pitch-yaw angle tests.

The pitch angle test results show that for roof separations between  $\frac{S}{D_j}$  values of 0 and

$$\frac{H}{D_j} - \frac{2}{2}$$

0.27 the most efficient installation occurred between  $5^\circ$  and  $10^\circ$  pitch. The  $0^\circ$  pitch tests showed lower installation efficiency due to greater frictional losses as the jet plume has greater contact with the tunnel roof. At larger pitch angles of  $10^\circ$  and  $15^\circ$  however, lower installation efficiencies are due to the jet plumes increasing contact with the tunnel floor.

At the wall-roof corner a 10° pitch/yaw proved most efficient at lower separation values. However, as separation increased lower pitch/yaw angles were more efficient. With the potential frictional losses due to the jet plumes corner location the optimum installation efficiency presumably occurs with a combination of increased separation and reduced pitch/yaw (2).

For the data gathered in this experiment the effect of the jet being adjacent to the wall was a 12% loss in installation efficiency relative to the centre line value. The effect of the jet being adjacent to the wall-roof corner was a 23% loss in installation efficiency relative to the centre line value. This is true for all hub-tip ratios with jet momentum and swirl.

## 5. Conclusions

The project set out to establish the effects of jet swirl, annular jet configuration and inclination on the installation efficiency (based on jet x-momentum) of a simulated jet fan outer plane. In order to compare installation efficiencies for a variety of jet configurations an assumption of 100% efficiency was made for a jet without a centre body positioned at the centre of the tunnel entry portal.

Three sets of swirl tests were conducted, all for a hub-tip ratio of 0.25 (16 mm centre body) having mean exit swirl angles of 0°, 17° and 30°. No discernible effect of swirl on installation efficiencies was found for these tests. At present there is no evidence that a swirling jet diffuses x-momentum more efficiently into the secondary flow or that secondary flow entrainment is in any way enhanced.

The increase in jet momentum, created by increasing the jet centre body diameter and maintaining a constant jet mass flow, resulted in an efficiency drop at all separations from tunnel roof and wall-roof corner. The decrease in efficiency at the roof was consistent with increased frictional shear, however the decrease at the tunnel centre was unexpected and thought due to annular jet filling in and diffusing rapidly towards the jet centre line before diffusing completely into the secondary flow. The nominal jet velocity could therefore be considered lower than the simple annular jet value bringing the effective installation efficiency back up to 100% for the equivalent plane jet.

The pitch angle tests at the tunnel roof showed a maximum installation efficiency with the jet inclined between 5° and 10°. At the wall-roof corner the highest installation efficiency occurred at an average 10° pitch/yaw jet configuration for the lower separation values. However, increased separation resulted in increased installation efficiencies at lower pitch/yaw angles.

The experimental data recorded from all tests was normalised and the relative installation efficiencies for each jet configuration for all variations of momentum and swirl were plotted. This clearly shows a significant increase in installation efficiency is gained by inclining the jet away from its adjacent surface or surfaces.

## 6. References

- (1) Armstrong, J., Bennett, E.C. & Matthews, R.D. "Three-Dimensional Flows in a Circular Tunnel due to Jet Fans" Proceedings of the 8th International Symposium on Aerodynamics and Ventilation of Vehicle Tunnels, Mechanical Engineering Publications, London, 1994, pp 743 - 756
- (2) Tabarra, M., Bennett E.C., Matthews R.D., Armstrong, J., Smith T.W. "Eccentricity Effects on Jet Fan Performance in Longitudinally Ventilated Rectangular Tunnels." Fans For Hazardous Applications, Papers presented at an IMechE Seminar, Mechanical Engineering Publications, London, 1994 pp 11 - 16
- (3) British Standards Institute, "Measurement of Fluid Flow in Closed Conduits." BS 1042 : Section 1.1 : 1981

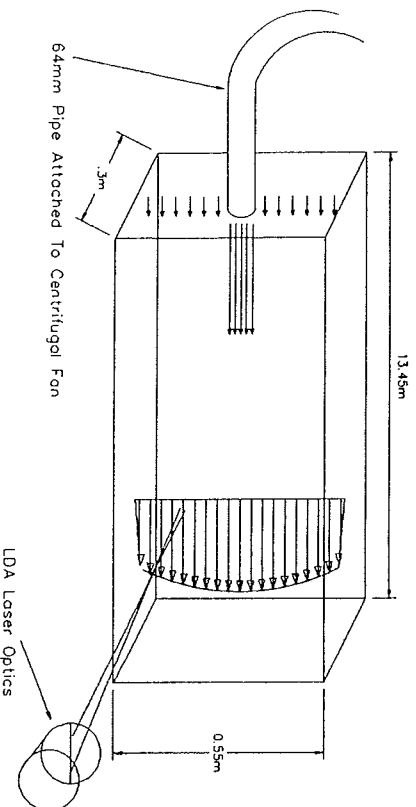


Figure 1. Schematic of Experimental Rig

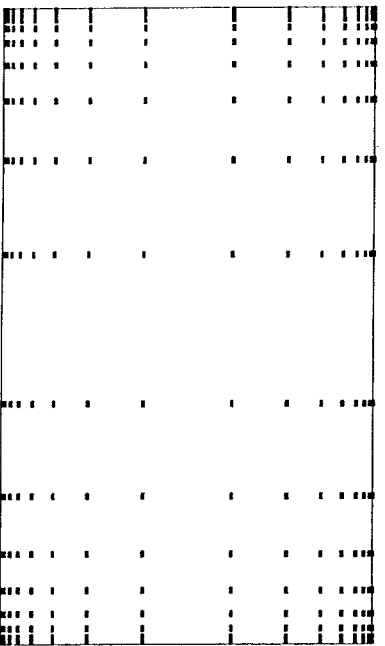


Figure 2. Laser Doppler Anemometer Point Traverse Grid (0.3m x 0.55m)

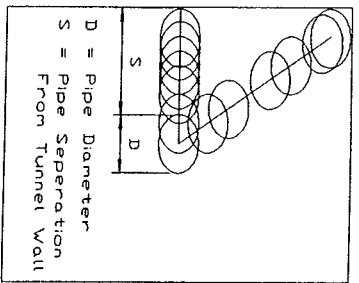


Figure 3. Pipe Positions for Eccentricity Tests (0.3m x 0.55m tunnel shown on its side).

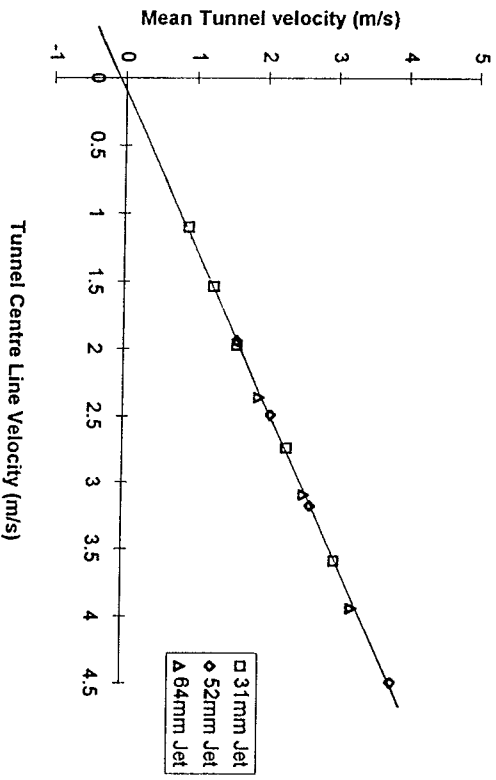


Figure 4. Relationship of Tunnel Centre line Velocity and Mean Tunnel Velocity

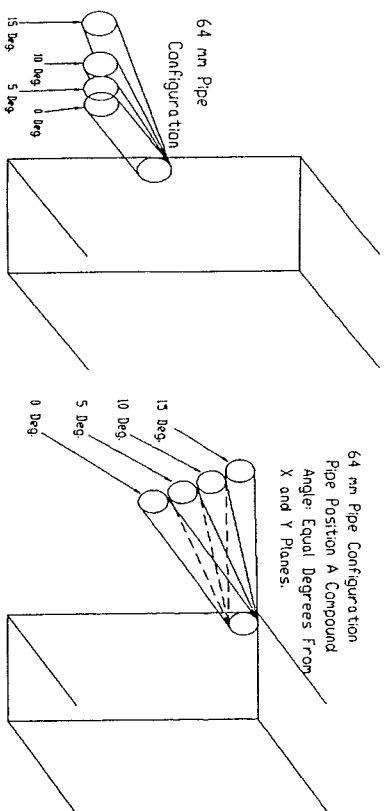


Figure 5a. Inclination of Pipe from Tunnel Roof

Figure 5b. Inclination of Pipe from Tunnel Wall/Roof Corner

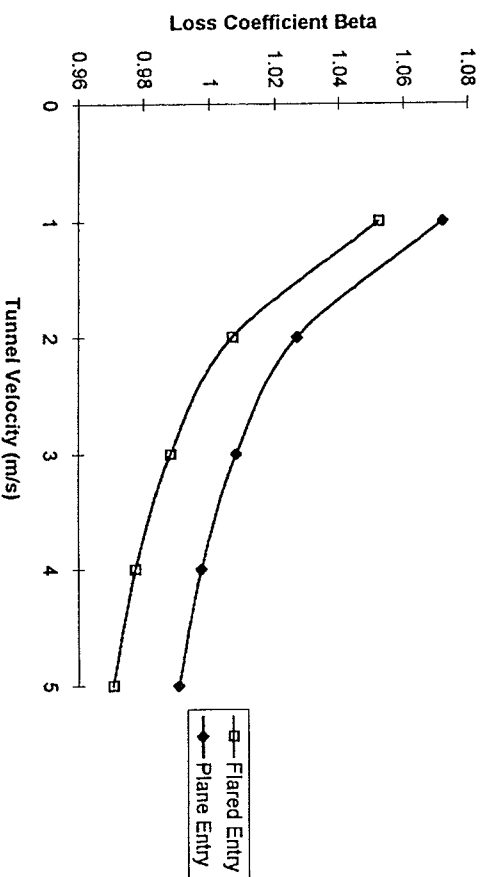


Figure 6. Relationship of Tunnel Loss Coefficient "Beta" and Tunnel Velocity

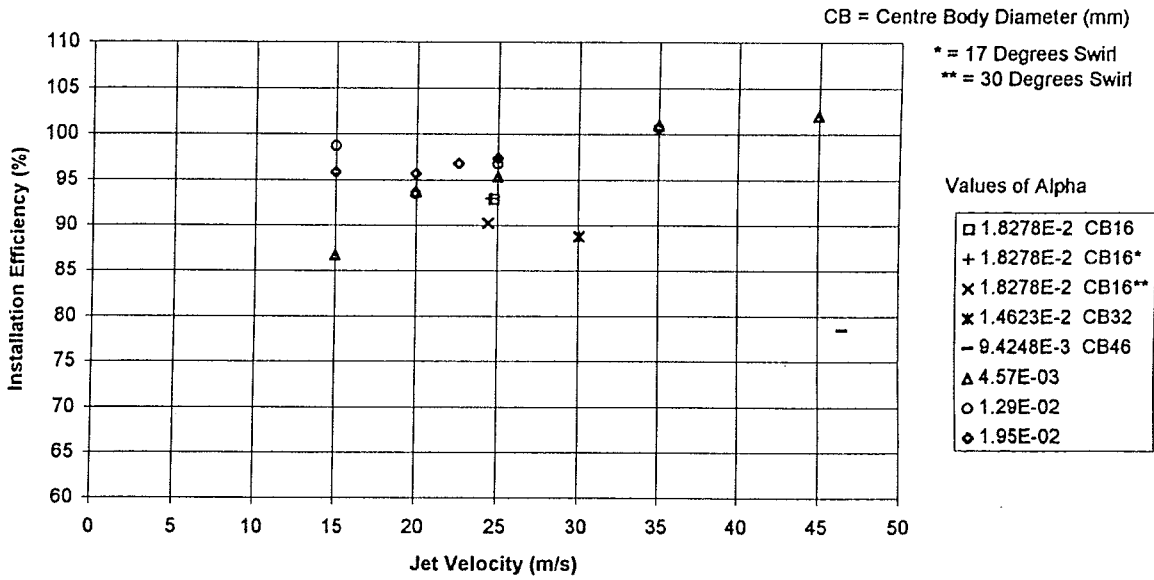


Figure 7. Relationship of Jet Velocity and Installation Efficiency

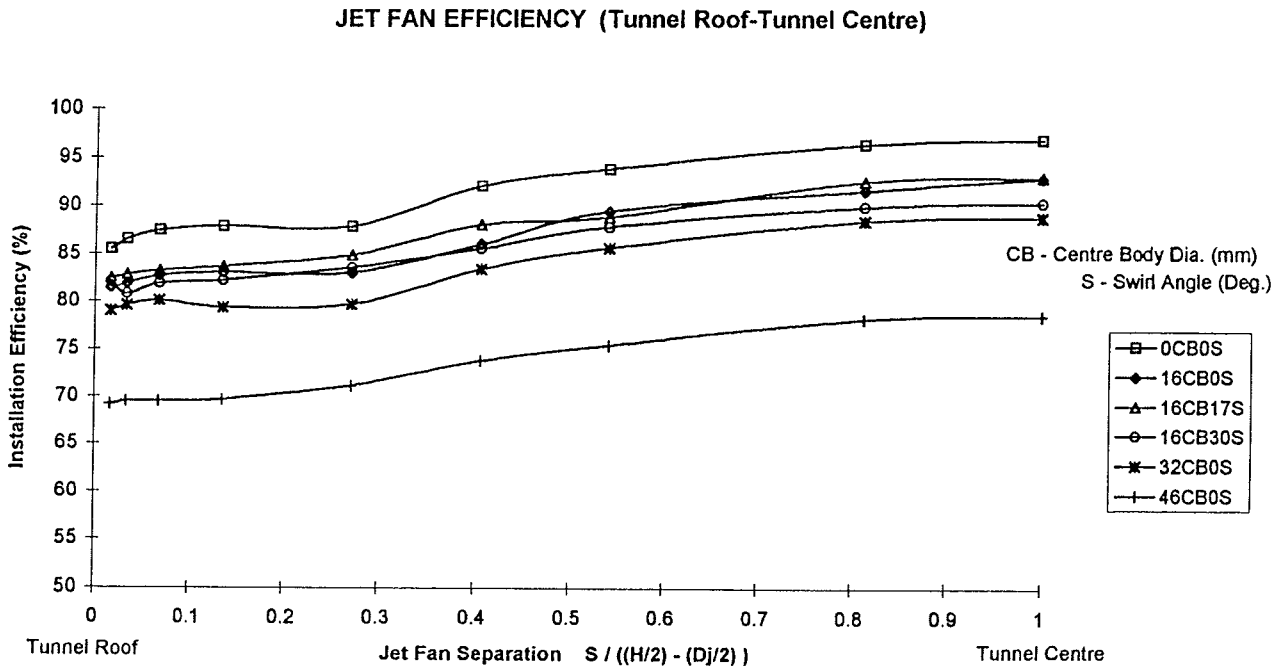


Figure 8. Jet Separation from Tunnel Roof to Tunnel Centre



### JET FAN INSTALLATION EFFICIENCY (Wall-Roof Corner - Tunnel Centre)

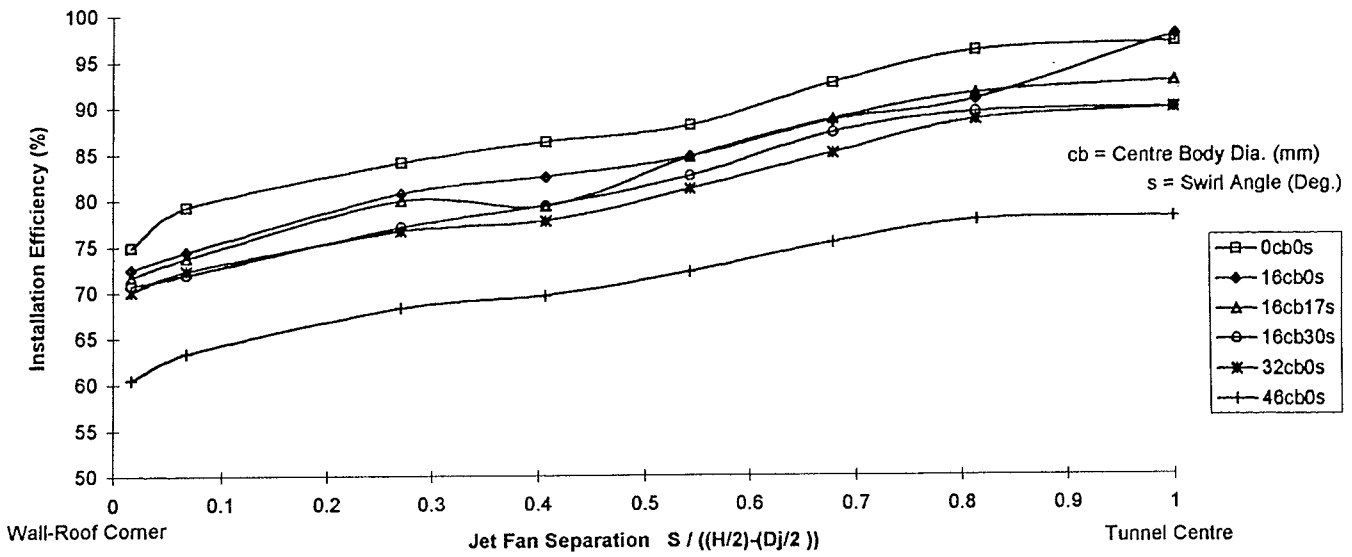


Figure 9. Jet Separation from Tunnel Wall/Roof Corner to Tunnel Centre

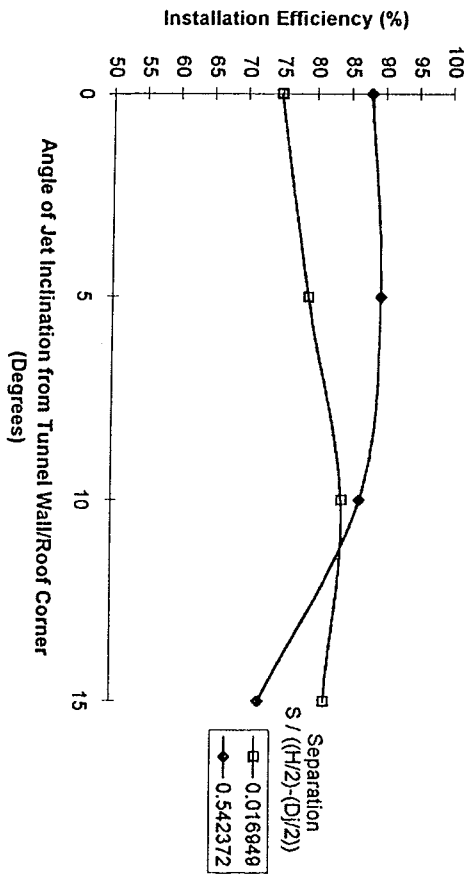


Figure 10. No Centre Body - No Swirl  
Effect of Jet Inclination from Tunnel Roof on Installation Efficiency

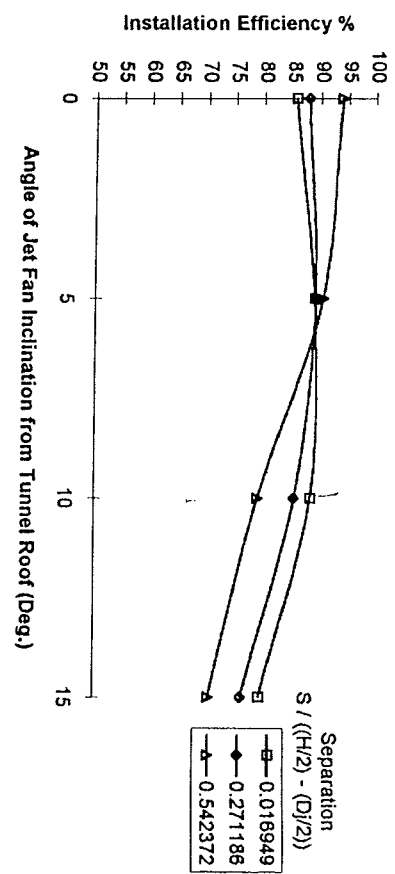


Figure 11. No Centre Body - No Swirl  
Effect of Jet Inclination from Tunnel Wall/Roof Corner on Installation Efficiency

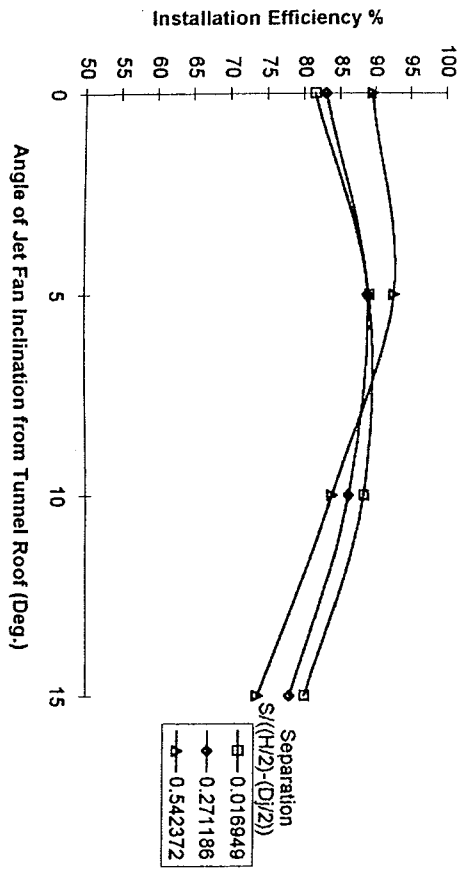


Figure 12. 16mm Diameter Centre Body - No Swirl  
Effect of Jet Inclination from Tunnel Roof on Installation Efficiency

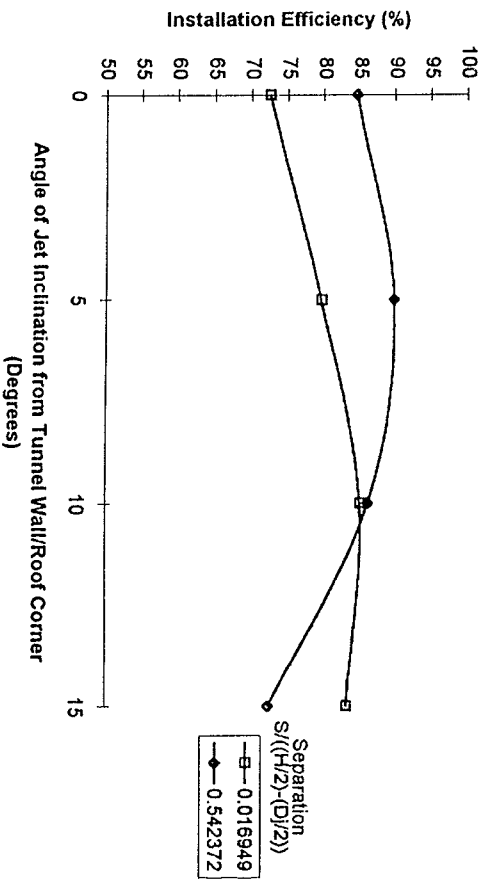


Figure 13. 16mm Diameter Centre Body - No Swirl  
Effect of Jet Inclination from Tunnel Wall/Roof Corner on Installation Efficiency

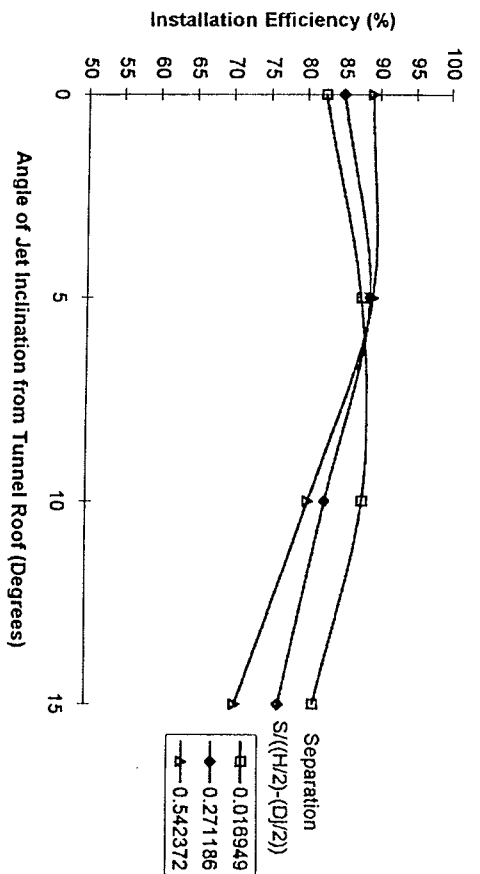


Figure 14. 16mm Diameter Centre Body - 17 Degrees Swirl  
Effect of Jet Inclination from Tunnel Roof on Installation Efficiency

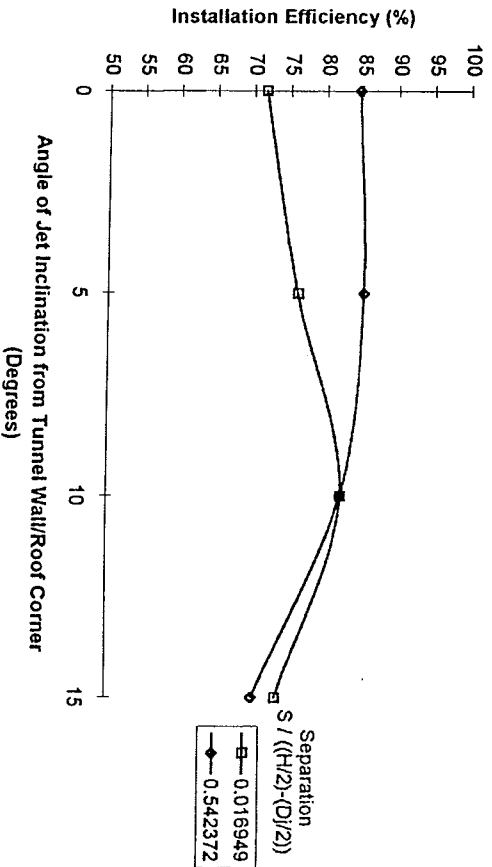


Figure 15. 16mm Diameter Centre Body - 17 Degrees Swirl  
Effect of Jet Inclination from Tunnel Wall/Roof Corner on Installation Efficiency

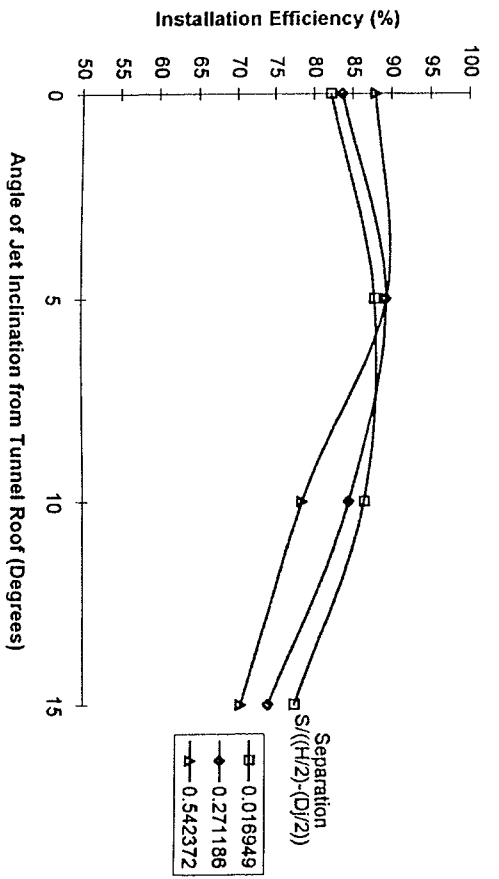


Figure 16. 16mm Diameter Centre Body - 30 Degrees Swirl  
Effect of Jet Inclination from Tunnel Roof on Installation Efficiency

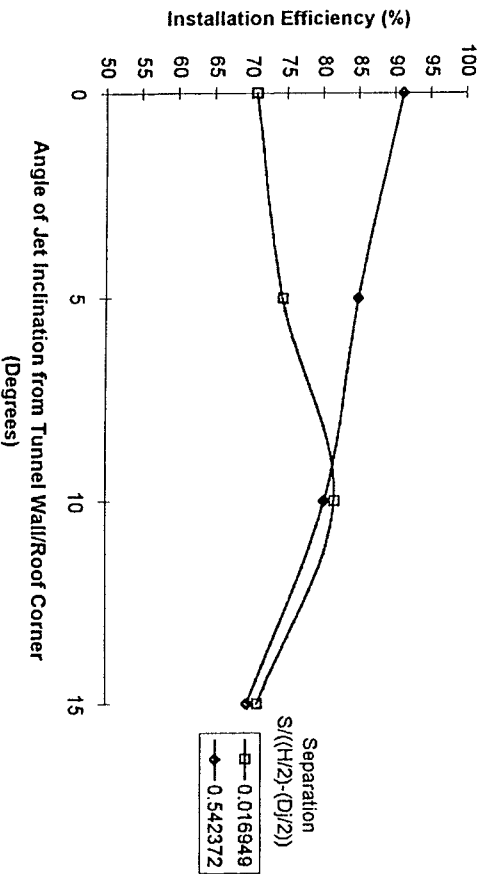


Figure 17. 16mm Diameter Centre Body - 30 Degrees Swirl  
Effect of Jet Inclination from Tunnel Wall/Roof Corner on Installation Efficiency

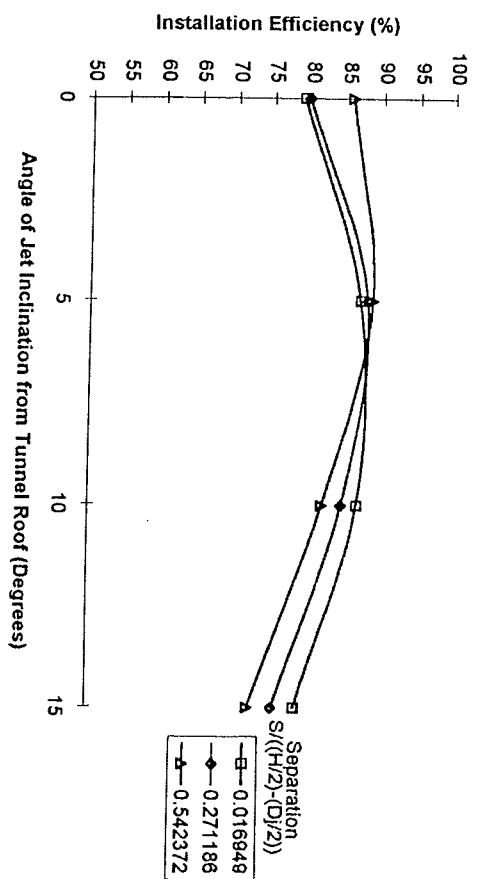


Figure 18. 32mm Diameter Centre Body - No Swirl  
Effect of Jet Inclination from Tunnel Roof on Installation Efficiency

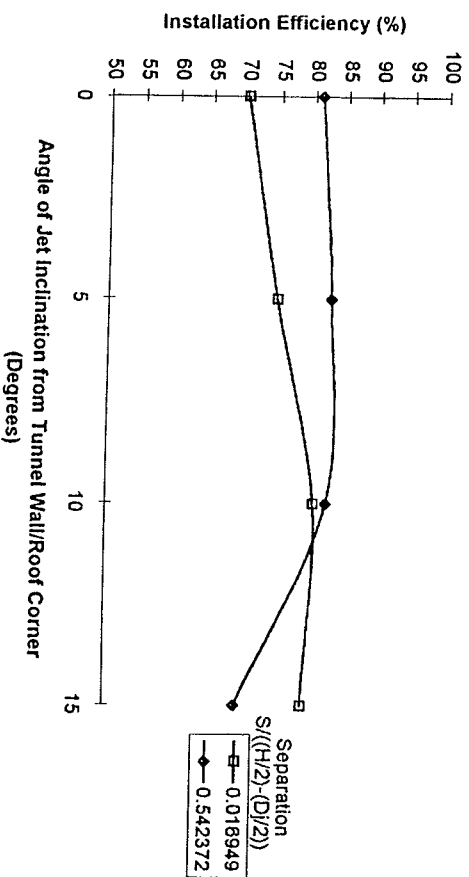


Figure 19. 32mm Diameter Centre Body - No Swirl  
Effect of Jet Inclination from Tunnel Wall/Roof Corner on Installation Efficiency

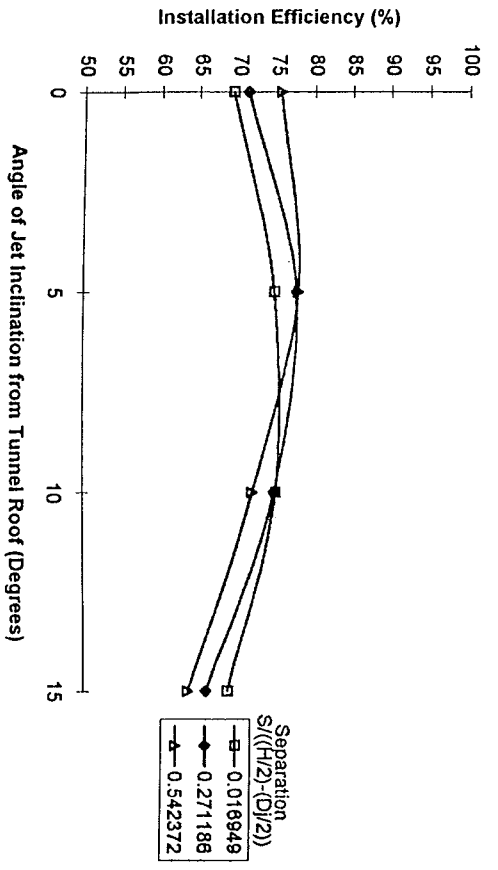


Figure 20. 46mm Diameter Centre Body - No Swirl  
Effect of Jet Inclination from Tunnel Roof on Installation Efficiency

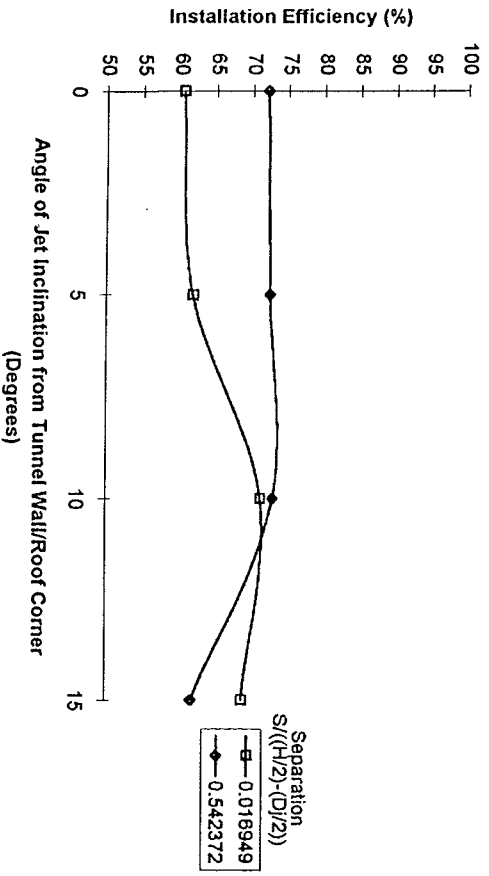


Figure 21. 46mm Diameter Centre Body - No Swirl  
Effect of Jet Inclination from Tunnel Wall/Roof Corner on Installation Efficiency

## Aerodynamics – Road II